POTSDAM-INSTITUT FÜR
KLIMAFOLGENFORSCHUNG

Modeling glacial-interglacial changes in global fire regimes and trace gas emissions

Kirsten Thonicke[1]
Max-Planck-Institute for Biogeochemistry, Jena, Germany

Potsdam-Institute for Climate Impact Research (PIK), Potsdam, Germany

I. Colin Prentice
Quantifying and Understanding the Earth System (QUEST), Department of Earth Sciences, University of Bristol, Bristol, UK

Chris Hewitt
Met Office, Hadley Centre, Exeter, UK

Received 6 April 2004; revised 14 March 2005; accepted 18 May 2005; published 29 July 2005.

[1] Climate at the Last Glacial Maximum (LGM) together with low atmospheric CO_2 concentration forced a shift in vegetation zones, generally favored grasses over woody plants and allowed the colonization of continental shelves. Many studies using models and/or palaeo data have focused on reconstructing climate and vegetation changes between LGM and present, but the implications for changes in fire regime and atmospheric chemistry have not previously been analyzed. We have investigated possible global changes in fire regime using climate model simulations of the LGM to drive the Lund-Potsdam-Jena Dynamic Global Vegetation Model (LPJ) with its embedded fire model, Glob-FIRM. Simulation results reveal a pronounced shift of pyrogenic emission sources to lower latitudes. Global total emissions were slightly reduced. Enhanced nitrogen oxides emissions in the tropics could potentially have increased the oxidizing capacity of the atmosphere, helping to explain the low atmospheric methane concentrations during glacial periods as observed in the ice core records.

Citation: Thonicke, K., I. C. Prentice, and C. Hewitt (2005), Modeling glacial-interglacial changes in global fire regimes and trace gas emissions, *Global Biogeochem. Cycles*, *19*, GB3008, doi:10.1029/2004GB002278.

1. Introduction

[2] Atmospheric methane (CH_4) concentration increased from ~350 ppbv at the Last Glacial Maximum (LGM, ~23 to 19 ka BP) to ~700 ppbv during the pre-industrial Holocene. If the atmospheric oxidizing capacity were unchanged, this difference would correspond to a change in CH_4 flux of ~330 Tg/yr from all sources [*Chappellaz et al.*, 1993]. However, modeling studies have found that changes in the distribution and productivity of wetlands cannot fully explain observed changes in CH_4. Despite a modeled 15% increase in global wetland area at the LGM relative to recent conditions, wetlands productivity was estimated to be 25% less than under present climate conditions; this corresponds to a net reduction of 33 Tg/yr in the CH_4 source [*Kaplan*, 2002], i.e., far too small a reduction to account for the glacial-interglacial change in CH_4 concentration in the atmosphere. The true extent of wetlands on the exposed continental shelves is an important issue requiring further research [*Wania et al.*, 2004]; however, offshore peat deposits of LGM age are known and must presumably have contributed to the global CH_4 budget [see, e.g., *Kaplan*, 2002, and references therein]. Changes in other CH_4 sources such as hydrates and permafrost soils have been hypothesized to contribute to low glacial CH_4 emissions, but it is difficult to account for large changes required by these mechanisms [*Kennett and Fackler-Adams*, 2000]. It is still an open question to what extent changes in vegetation distribution, atmosphere, and fire regimes could have affected the distribution of sources and sinks of CH_4. Such changes could have influenced atmospheric CH_4 either directly through changes in sources or indirectly by affecting the oxidizing capacity of the atmosphere, which depends on the sources and sinks of other reactive trace gases as well as CH_4.

[3] The climate at the LGM was characterized by generally lower temperatures, and in many regions by lower precipitation, than the climate of the Holocene (the present interglacial). Changes in the atmospheric concentrations of trace gases, coverage of ice, and ocean dynamics were associated with changes in the atmospheric circulation and climate [e.g., *Kageyama et al.*, 2001; *Pinot et al.*, 1999].

[1]Now at School of Geographical Sciences, University of Bristol, Bristol, UK.

0886-6236/05/2004GB002278

Table 1. Emission Factors for Deriving CO_2, CO, CH_4, VOC, TPM, and NO_x Emissions From Biomass Burnt Under Present Conditions, Which Were Implemented in LPJ as PFT Parameters[a]

	Emission Factor					
Plant Functional Type (PFT)	*CO_2*	*CO*	*CH_4*	*VOC*	*TPM*	*NO_x*
1: Tropical broadleaved evergreen woody	1580	103	6.8	8.1	8.5	1.85 (1.99)
2: Tropical broadleaved raingreen woody	1664	63	2.2	3.4	8.5	2.35 (2.54)
3: Temperate needleleaved evergreen woody	1568	106	4.8	5.7	17.6	3.0 (3.24)
4: Temperate broadleaved evergreen woody	1568	106	4.8	5.7	17.6	3.0 (3.24)
5: Temperate broadleaved summergreen woody	1568	106	4.8	5.7	17.6	3.0 (3.24)
6: Boreal needleleaved evergreen woody	1568	106	4.8	5.7	17.6	3.0 (3.24)
7: Boreal broadleaved summergreen woody	1568	106	4.8	5.7	17.6	3.0 (3.24)
8: C_3 perennial grass	1568	106	4.8	5.7	17.6	3.0 (3.24)
9: C_4 perennial grass	1664	63	2.2	3.4	8.5	2.35 (2.54)

[a]See *Andreae and Merlet* [2001]. VOC is volatile organic carbon, TPM is total particulate matter, and PFT is plant functional types. Emissions are given in gram species per kilogram dry matter burnt. Emission factors given for NO_x are lower for savannah and grasslands than previous publications. Other updates revealed only minor changes (M. O. Andreae, personal communication, 2003). The emission factor for NO_x as adjusted to carbon-to-nitrogen ratio of the Last Glacial Maximum (+8%) is shown in parantheses. Savannah and grasslands correspond to PFT 2 and 9, tropical forests correspond to PFT 1, and extratropical forests correspond to PFT 3 to 8.

The LGM climate, together with an atmospheric CO_2 concentration of <200 ppm, forced a southward shift of boreal and temperate vegetation, generally favored grasses over woody plants, and allowed the colonization of continental shelves due to the decreased sea level [*Labeyrie et al.*, 2003]. Low atmospheric CO_2 concentration also tends to favor C_4 over C_3 plants owing to reduced photosynthesis of C_3 plants as a consequence of reduced substrate concentration and reduced competition by O_2 for the Rubisco carboxylation sites [*Cowling and Sykes*, 1999, 2000; *Polley et al.*, 1993]. Owing to the advantage of C_4 photosynthesis in carbon gain at high temperatures and low atmospheric CO_2 concentration, C_4 grasses are likely to have expanded greatly at the expense of C_3 grasses and of woody plants in the tropics [*Collatz et al.*, 1998; *Harrison and Prentice*, 2003].

[4] Burning conditions are driven by climate and vegetation status (including fuel moisture and amount). Fire has implications for vegetation dynamics, biogeochemical cycles, atmospheric chemistry, and radiative forcing. Changes in climate affect vegetation composition and its productivity, resulting in different patterns of global fire regimes. Much work has been done on reconstructing climate and vegetation changes between LGM and the present, and on the causes of millennial-scale variability during the glacial period, but the potential implications for changes in fire regime and atmospheric chemistry have not previously been analyzed.

[5] Little is known about how different fire regimes worldwide were at the LGM as only relatively few time series of reconstructions or lake sediment histories date back to that time, and the existing data have not been compiled in any synthetic form. A number of reconstructions for North America indicate reduced fire activity during the late-glacial and early Holocene (17–12 ka BP). There is evidence for increased fire during warm/dry periods during the Holocene, sometimes reflecting interactions with changing vegetation composition depending on the different fire-sensitivity of different plant types [*Anderson and Smith*, 1997; *Brunelle and Whitlock*, 2003; *Hallett et al.*, 2003; *Millspaugh et al.*, 2000; *Winkler*, 1997; *Bradshaw et al.*, 1997]. Analysis of a marine core in the Banda Sea, Southeast Asia, indicated drier and colder conditions during the last two glacial periods in eastern Indonesia and northern Australia, reflected by expansion of lower montane forests and higher charcoal and elemental carbon values suggesting increased burning during these periods [*van der Kaars et al.*, 2000]. Exposure of continental shelves, atmospheric circulation pattern, and high climate variability also control fire frequency in the tropics, where reconstruction revealed patterns for Southeast Asia different from those for Central and South America (17–12 kyr BP [*Haberle et al.*, 2001; *Haberle and Ledru*, 2001]). Analysis of charred grass cuticles outlined the importance of grassland fires at Mount Kenya during the LGM and indicated high fire occurrence in African savannahs [*Wooller et al.*, 2000].

[6] This coincidence of changes in fire occurrence with changing climate and associated vegetation composition is indirectly supported by measurements of ammonium (NH_4^+) concentrations in Greenland Ice cores. Owing to the atmospheric lifetime of ammonium (about a week) and the prevailing atmospheric circulation pattern, changes in NH_4^+ in Greenland have been attributed to changing biogenic sources in North America, i.e., soil, vegetation and biomass burning [*Fuhrer et al.*, 1996]. Owing to its relatively low (15%) contribution to overall deposition, the possibility to use NH_4^+ as a fire proxy has been disputed [*Hansson and Holmen*, 2001]. Changes in NH_4^+, however, seem to indicate less fire activity in the Northern Hemisphere, mainly North America, that changed in conjunction with reduced biogenic activity in the area at the LGM.

[7] We have investigated possible global changes in fire regime using climate model simulations of the Last Glacial Maximum (LGM) to drive the Lund-Potsdam-Jena Dynamic Global Vegetation Model (LPJ) [*Sitch et al.*, 2003]. Its embedded fire regime model Glob-FIRM [*Thonicke et al.*, 2001] predicts changes in fire regime as a complex interaction between vegetation productivity, carbon cycling, and ecosystem water balance. Climate data sets from 17 Palaeoclimate Modeling Intercomparison Project (PMIP) Phase I atmospheric General Circulation Models (GCMs) and from

Table 2. Influence of Carbon-to-Nitrogen (C:N) Ratio on Carbon Pools and Fluxes [PgC] Under Pre-Industrial and Last Glacial Maximum (LGM) Climate[a]

Simulation Experiment	Vegetation Carbon				Annual Net Primary Production (NPP)				Annual Heterotrophic Respiration R_h				Biomass Burnt			
	Absolute Value, PgC	Effect of C:N Ratio Under Same Climate, %	Effect of Climatic Change Only, %	Effect of Both Climate and C:N Ratio, %	Absolute Value, PgC	Effect of C:N Ratio Under Same Climate, %	Effect of Climatic Change Only, %	Effect of Both Climate and C:N Ratio, %	Absolute Value, PgC	Effect of C:N Ratio Under Same Climate, %	Effect of Climatic Change Only, %	Effect of Both Climate and C:N Ratio, %	Absolute Value, PgC	Effect of C:N Ratio Under Same Climate, %	Effect of Climatic Change Only, %	Effect of Both Climate and C:N Ratio, %
Pre-Industrial Climate																
Contemporary C:N ratio	746				55.3				51.5				3.8			
C:N ratio −8%	706	−5.2			53.9	−2.5			50.5	−2.0			3.4	−9.4		
LGM Climate (HadCM3)																
Contemporary C:N ratio	495		−33.6		45.7		−17.5		42.4		−17.7		3.2		−14.1	
C:N ratio −8%	470	−5.1		−37.0	44.7	−2.1		−19.2	41.8	−1.3		−18.8	2.8	−12.3		−24.6

[a]Effects of different C:N ratios under similar climate conditions and effects of changes in climate and the C:N ratio are given in percentages. The changes in the C:N ratio have a similar reductive effect on vegetation carbon, productivity (NPP), and heterotrophic respiration (R_h) under both climates, but are largest on biomass burnt under LGM climate. Maximal reductions result from the combination of different climate conditions and a reduced C:N ratio in all pools and fluxes, with vegetation carbon as the highest, followed by biomass burning.

the Hadley Centre coupled ocean-atmosphere general circulation model HadCM3, all describing LGM climate conditions, were applied and compared against pre-industrial climate conditions.

2. Methods and Data

[8] Monthly anomaly fields of temperature, precipitation, and fractional sunshine hours were derived from all 17 PMIP I atmospheric GCMs and the coupled ocean-atmosphere GCM HadCM3. These anomalies were applied to the multiyear CRU climatology, provided by the Climate Research Unit (CRU), University of East Anglia, UK ($0.5° \times 0.5°$, 1901–2000), to obtain a 30-year LGM climatology with interannual climate variability. Boundary conditions for the PMIP I GCMs and their model characteristics are documented by *Harrison and Prentice* [2003]. The model's ability to simulate climate at the LGM was analyzed by *Pinot et al.* [1999] for Europe and western Siberia and *Kageyama et al.* [2001] for tropical palaeoclimates.

[9] The PMIP I GCMs were either atmospheric GCMs forced with CLIMAP sea surface temperatures (SSTs) or atmospheric GCMs coupled to a simple one-layer thermodynamic (''slab'') ocean model with no ocean dynamics. The slab model, designed to provide a simple representation of the ocean mixed layer, allows SSTs to be interactively calculated in the GCM, but the lack of ocean dynamics and deep ocean restricts the feedbacks that can operate between the atmosphere and ocean. The HadCM3 model allows more feedbacks to operate by coupling an atmospheric GCM to a three-dimensional dynamic ocean general circulation model which models both the mixed layer and the deep ocean. The coupled ocean-atmosphere GCM (HadCM3) and its LGM simulation are described in more detail by *Hewitt et al.* [2003]. The model was forced with the same boundary conditions as the PMIP I GCMs.

[10] All LGM climate data sets were adjusted to the LGM land mask, which reflects exposure of continental shelves due to lower sea levels as well as the ice coverage in the Northern Hemisphere as reconstructed by *Peltier* [1994]. A value of 200 ppm was used as the constant atmospheric CO_2 concentration throughout the simulation time. In the pre-industrial control simulation, experiments under pre-industrial climate conditions were run for the contemporary land mask by using the climate data of the first 30 years of the CRU climatology and an atmospheric CO_2 concentration of 280 ppm.

[11] LPJ [*Sitch et al.*, 2003] simulates plant physiological processes and vegetation dynamics at daily to annual time steps. Nine Plant Functional Types (PFTs) are assigned bioclimatic, phenological, and physiognomic characteristics. The simulation of the water balance in LPJ was modified for this study to account for evaporation from bare soil, for interception, and for the consequences of the uneven temporal distribution of precipitation. These additions improved the simulation of soil moisture and runoff in major river catchments [*Gerten et al.*, 2004]. LPJ requires a climate input data set including interannual climate variability, soil texture information, and a prescribed atmospheric CO_2 concentration. Its embedded global fire model Glob-FIRM

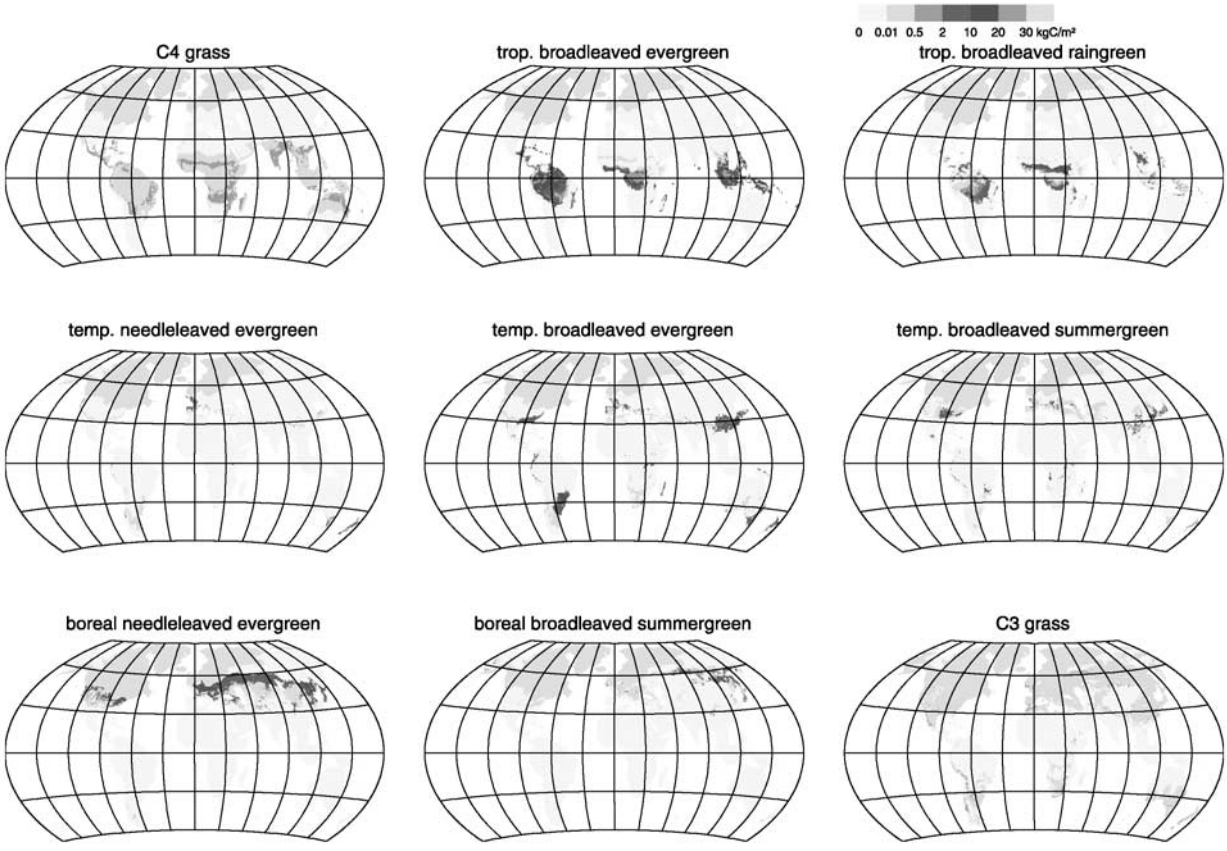

Figure 1. Carbon stored in aboveground, living biomass by Plant Functional Type (PFT). Pale blue region indicates ice. LPJ simulation uses the HadCM3 Last Glacial Maximum climate. See color version of this figure at back of this issue.

simulates global fire regimes as a complex interaction between vegetation productivity, carbon cycling, and ecosystem water balance. The model can describe broad features of the fire in both temperature- and moisture-limited ecosystems under present-day climate conditions [*Thonicke et al.*, 2001]. In order to estimate trace gas emissions, PFT-specific emission factors for major reactive trace gases were implemented into LPJ as PFT parameters (see Table 1). Thus changes in vegetation composition would have immediate consequences for simulated fire emissions.

[12] Contemporary C:N ratios are computed in LPJ based on optimal allocation theory [see *Sitch et al.*, 2003, equation (22)]. Changes in atmospheric CO_2 concentration affect the amount of carbon stored in plant tissues. Experimental data on changes in the C:N ratio of plant tissues indicate a reduction by about 8% at atmospheric CO_2 concentrations of 200 ppm [*Cowling and Sage*, 1998]; therefore C:N ratios for all living compartments of C_3 PFTs were adjusted accordingly. Consequently, burning the same amount of biomass at low atmospheric CO_2 concentration must result in higher NO_x emissions. We therefore increased the emission factor for NO_x by 8% for the LGM climate experiments. The sensitivity of vegetation productivity and carbon fluxes to this change in C:N ratio was tested by applying contemporary and LGM C:N ratios to pre-industrial and LGM climate (HadCM3), respectively. Thus the effects of climate, of atmospheric CO_2 concentration, and of C:N ratio could be quantified. Changing the C:N ratio had about the same effect on vegetation carbon storage under pre-industrial climate conditions with 280 ppm atmospheric CO_2 concentration as under LGM climate conditions and 200 ppm CO_2 (−5%; see Table 2). Global biomass burning was reduced by 9% under pre-industrial conditions, and by 12% under LGM climate conditions. Effects on net primary production and heterotrophic respiration were very small under similar climate conditions and changed at the same rate with changing both climate and the C:N ratio. Vegetation carbon storage decreased by 37% with the adjusted C:N ratio under LGM climate as compared to 33% without the adjustment. Thus the effect of changing C:N ratios is small but not negligible. In what follows we report results based on adjusted C:N ratios, including the effects on both vegetation dynamics and on the emission factor for NO_x.

3. Results and Discussion

3.1. Vegetation Dynamics and Carbon Storage

[13] Simulated carbon storage of the terrestrial biosphere (vegetation, litter, and soil) increased from 1640 PgC at the

Table 3. Global Estimates of Simulated Carbon Fluxes (±1 SD) and Trace Gas Emissions, for the Last Glacial Maximum Climatologies and Pre-Industrial Climate[a]

Simulation Experiment/Validation	Vegetation Carbon, PgC	Annual NPP, PgC	Annual R_h, PgC	Biomass Burnt, PgC	CO_2, Pg	CO, Pg	CH_4, Pg	VOC, Pg	TPM, Pg	NO_x, Tg
LGM PMIP I slab ocean	433 ± 28.3	41.5 ± 2.0	38.8 ± 1.9	2.6 ± 0.2	9.299	0.532	0.028	0.035	0.063	
LGM PMIP I prescribed SST	416 ± 20.7	41.3 ± 1.0	38.8 ± 0.9	2.5 ± 0.1	8.757	0.503	0.027	0.033	0.060	
LGM HadCM3	470	44.7	41.8	2.8	10.134	0.584	0.031	0.039	0.069	15.777
Pre-industrial control-run	746	55.3	51.5	3.8	13.480	0.758	0.037	0.046	0.101	20.787
Modern estimates				3.9	13.400	0.680	0.041	0.056	0.074	16.518
[*Andreae and Merlet*, 2001] (M. O. Andreae, personal communication, 2003)										

[a]Modern estimates of biomass burning are also given. SST is sea surface temperature, NPP is net primary production, and R_h is heterotrophic respiration.

LGM (applying the HadCM3 climate data set) to 2250 PgC under pre-industrial climate conditions, a difference of 610 PgC. Applying the PMIP I GCM climate data sets resulted in simulated carbon storage ranging between 1200 and 1600 PgC at the LGM with an average of 1460 PgC. These results agree with other modeling studies, observations, and reconstructions that the terrestrial biosphere stored about 300 to 700 PgC more carbon during interglacial than during glacial periods [see, e.g., *Bird et al.*, 1994; *Kaplan et al.*, 2002; *Joos et al.*, 2004].

[14] The simulated LGM vegetation distribution (HadCM3) shows reduced spatial coverage of woody vegetation types, widespread grasslands in dry/cold regions of the continents. Colder and drier conditions in the tropics increased grassland/xerophytic wood and shrub vegetation at the expense of forests (Figure 1, top). This feature is consistent with reconstructions of drought-tolerant vegetation types at sites where tropical rain forest is found under modern climate conditions, for example, in East Africa [*Prentice and Jolly*, 2000]. The drier and colder conditions in the tropics, together with lowered atmospheric CO_2 concentration, force an increase in grass cover and productivity at the expense of woody vegetation in the tropics. The simulated equatorward shift of boreal trees and the reduced area they occupied is broadly in agreement with pollen and macrofossil reconstructions for the LGM [*Harrison and Prentice*, 2003] (Figure 1, bottom). However, in Europe, boreal forest is simulated close to the Fennoscandian ice sheet, which is in contradiction to pollen reconstructions [*Prentice et al.*, 2000]. The GCM does not simulate temperatures as cold as proxy records suggest over western and central Europe. This problem is also found in the PMIP I GCMs [*Pinot et al.*, 1999], but some GCMs allowed the simulation of a zone of nonwooded vegetation around the Fennoscandian ice sheet (data not shown; see also *Harrison and Prentice* [2003] for PMIP

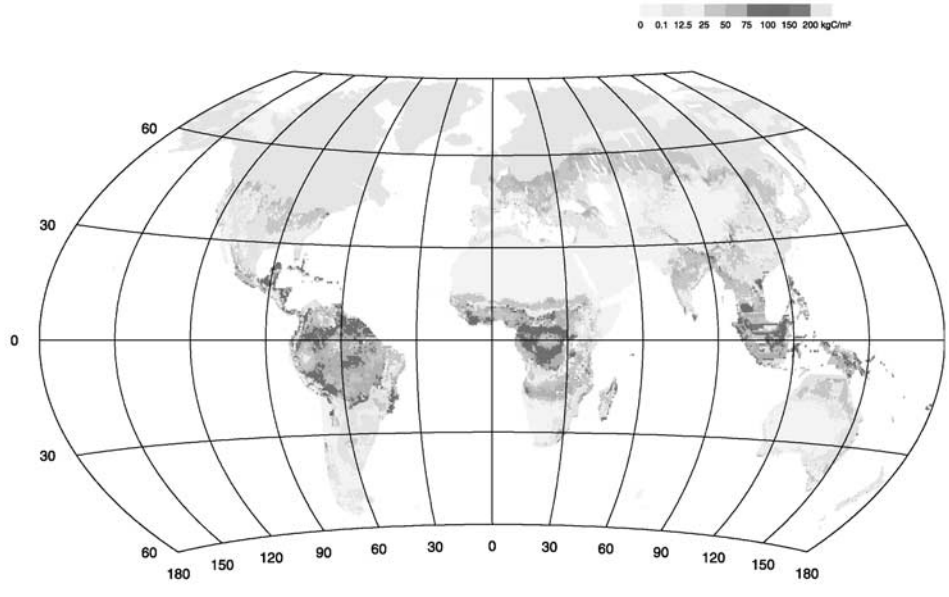

Figure 2. Simulated biomass burnt in the HadCM3 Last Glacial Maximum climate. Pale blue region indicates ice. See color version of this figure at back of this issue.

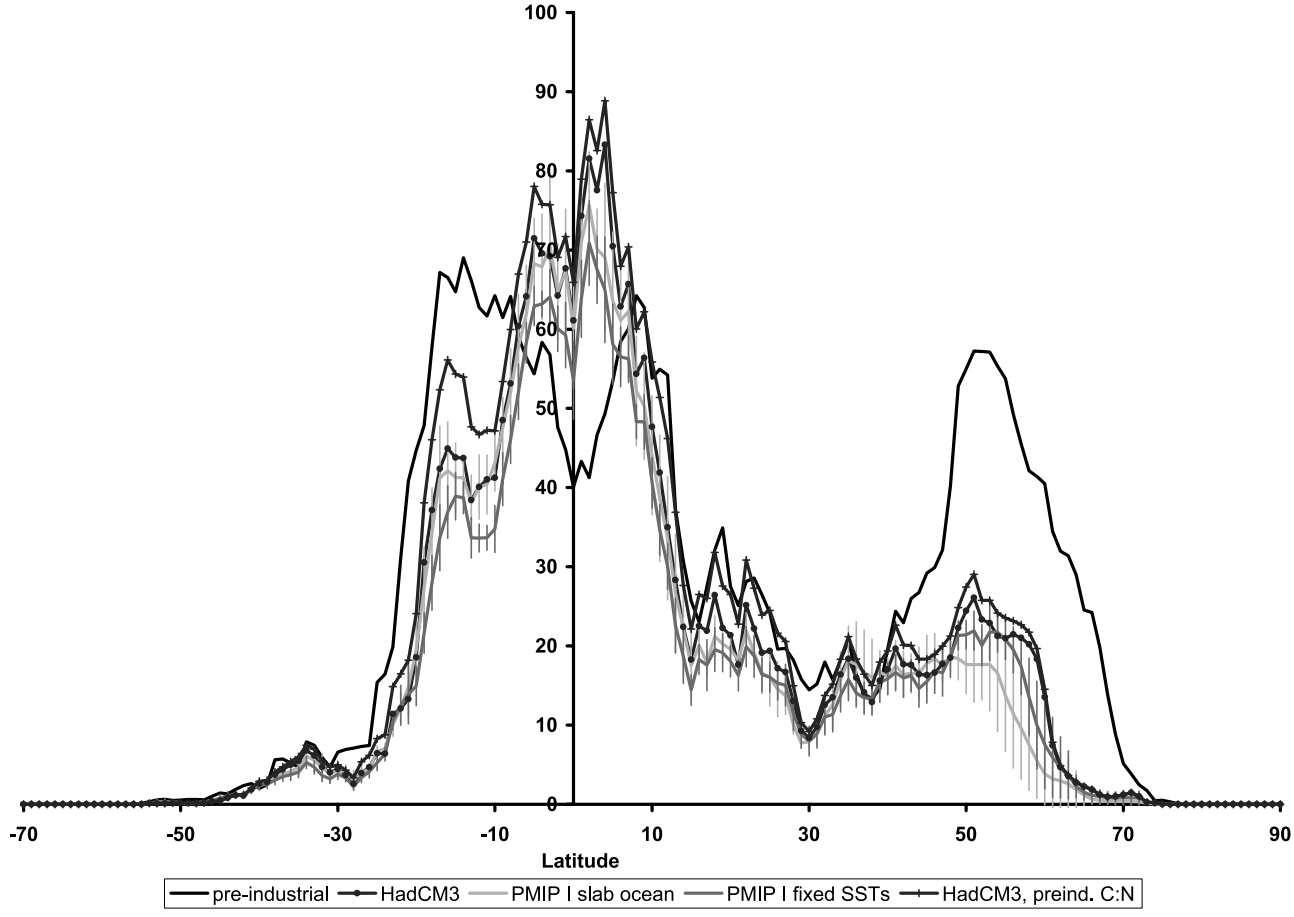

Figure 3. Latitudinal distribution of biomass burnt (*y* axis: sum by latitude bands in TgC/yr) under pre-industrial and Last Glacial Maximum (LGM) climate conditions (Palaeoclimate Modeling Intercomparison Project Phase I (PMIP I) GCMs with slab ocean, PMIP I GCMs with fixed sea surface temperatures, HadCM3 with C:N ratio adjusted to atmospheric CO_2 concentration at LGM and with C:N ratio under pre-industrial conditions). Bars indicate standard deviation among PMIP I GCM runs.

applications of the BIOME4 model). The simulation of the boreal forests in North America close to the Laurentide ice sheet, however, is confirmed by biome reconstructions [*Jackson et al.*, 2000; *Prentice and Jolly*, 2000; *Williams et al.*, 2000]. As a consequence of the equatorward shift of the boreal forest and the expansion of nonwooded vegetation due to climate and atmospheric CO_2 content, the temperate forest was also simulated as restricted and fragmented areas in Europe and as a continuous zone south of the boreal forest in North America (compare Figure 1 middle and bottom panels).

3.2. Changes in Biomass Burning

[15] Simulation results for biomass burning and trace gas emissions under pre-industrial conditions are in good agreement with modern estimates (Table 3). Simulated biomass burning at the LGM was largest in the tropical zone with biomass burning also occurring in tropical savannahs and in the boreal forest (Figure 2). Cold/dry regions with sparse or no vegetation show little or no biomass burning.

[16] Comparison between pre-industrial and LGM climate simulations shows a small reduction in global emission at LGM, but also a pronounced latitudinal shift (Table 3 and Figure 3). This is a surprising result, since it was not known how regional climate conditions and changed vegetation productivity would have affected burning conditions, i.e., heat, dryness, and fuel load, and thus global fire regimes at the LGM. In the contrary, reduced burning at mid- to high-northern latitudes is nearly slightly compensated by increased burning in the tropical zone. Biomass burning is shown as having a single (equatorial) maximum at the LGM, where under pre-industrial conditions a bi-modal distribution was simulated.

[17] Results in biomass burning using the HadCM3 GCM are in the upper range of the results from the PMIP I GCMs. The variability among the PMIP I GCMs is largest north of 50°N, i.e., indicating the difficulty simulating the climate around the ice sheets. GCMs with a slab ocean yielded a cooler climate in the Northern Hemisphere than the GCMs with prescribed sea surface temperature (SSTs), leading to lower simulated biomass burning. On the other hand, biomass burning emissions are higher in equatorial regions and neighboring low latitudes using the slab model results compared to those with fixed SSTs. There is agreement

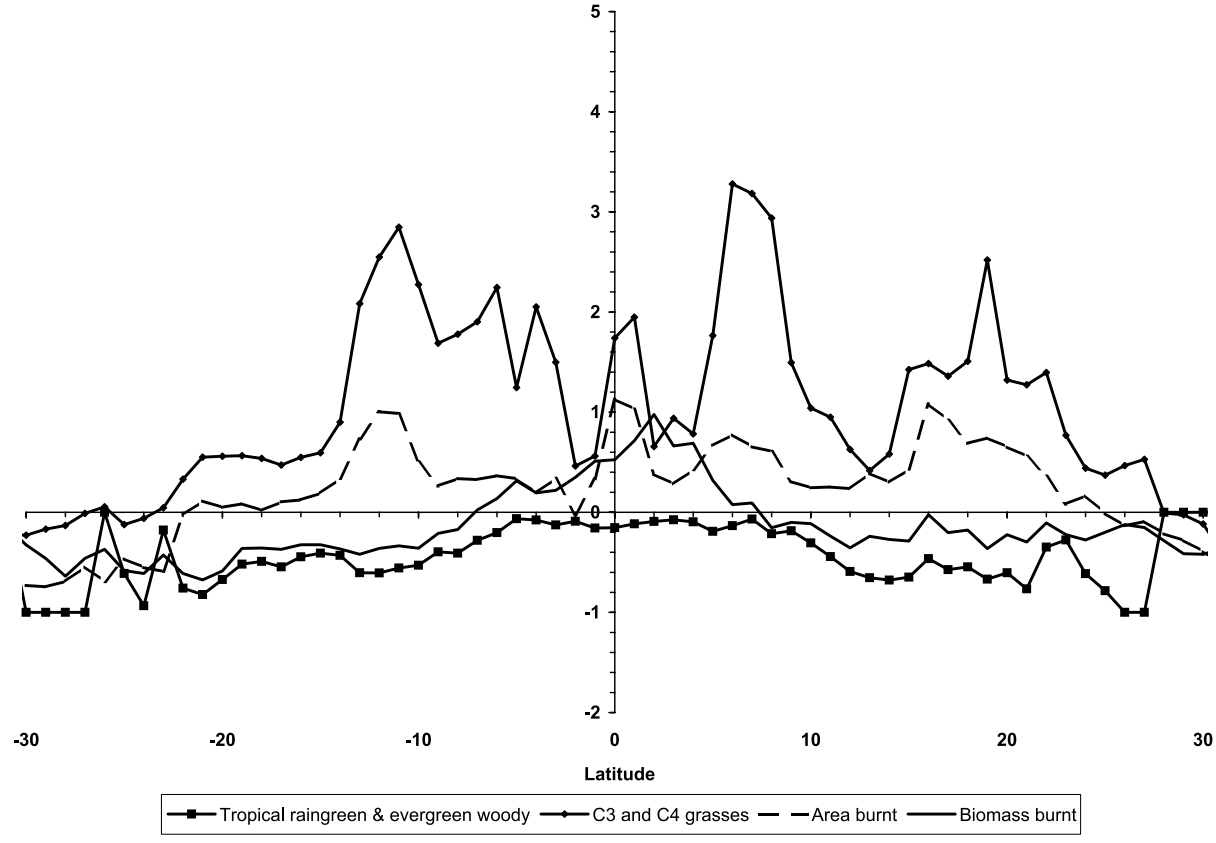

Figure 4. Relative changes in vegetation carbon stored by Plant Functional Type (PFT), area burnt, and biomass burnt relative to pre-industrial climate conditions using HadCM3 Last Glacial Maximum (LGM) climate. Positive values represent more carbon under LGM than under pre-industrial climate, and negative values represent the opposite. The change in area burnt corresponds broadly to changes in grass carbon storage, whereas the change in biomass burnt corresponds broadly to changes in vegetation carbon stored by tropical woody PFTs.

between all LGM GCMs in simulated biomass burning around 30°N and 30°S, corresponding to large extension of arid areas. Simulated changes in biomass burning are small between 40°N and 10°N, and south of 30°S but this is also where the largest effect of the C:N ratio appears, i.e., in the savannah/woodland zone, where the productivity of woody vegetation is marginal. Whereas the extension of the ice sheets in the Northern Hemisphere can mainly explain the reduction in biomass burning, it is the colonization of exposed continental shelves in the tropics and subtropics that determines an increase in biomass burning on the order of 10 to 30%, depending on the latitude, with an effect of 0.3 PgC globally.

[18] Less carbon was stored in the living biomass of tropical woody PFTs. The smallest simulated decrease was in the inner tropics, with a continuous increase toward the subtropics (see Figure 4 for relative changes in vegetation carbon stored per PFT with HadCM3 GCM application). At the same time the tropics also yield the largest biomass burning emissions at the LGM. Can changes in vegetation dynamics explain simulated changes in biomass burning? Latitudinal changes in area burnt, which result from changes in moisture conditions and in litter production, correspond to latitudinal changes in grass productivity, especially in the savannah regions and to a certain extent in the inner tropics. The total amount of biomass burning, which is a result of both area burnt and available biomass load of the PFTs present, is mainly driven by changes in the productivity of woody PFTs. Latitudinal changes in biomass burning coincide to a certain extent with changes in vegetation productivity of woody PFTs; that is, increases in area burnt do not automatically translate into increases in biomass burning, except for the inner tropics, where both factors (area burnt and grass productivity) determine the increase in simulated biomass burning (Figure 4).

3.3. Trace Gas Emissions

[19] The estimation of atmospheric trace gas emissions depends on emission factors, which differ among vegetation zones, but are assumed constant within any given zone owing to an implicitly fixed relationship between glowing and flaming combustion as defined for each vegetation zone (see Table 1). The partition of biomass burnt into major trace gases is assumed invariant (Figure 5). Global estimates

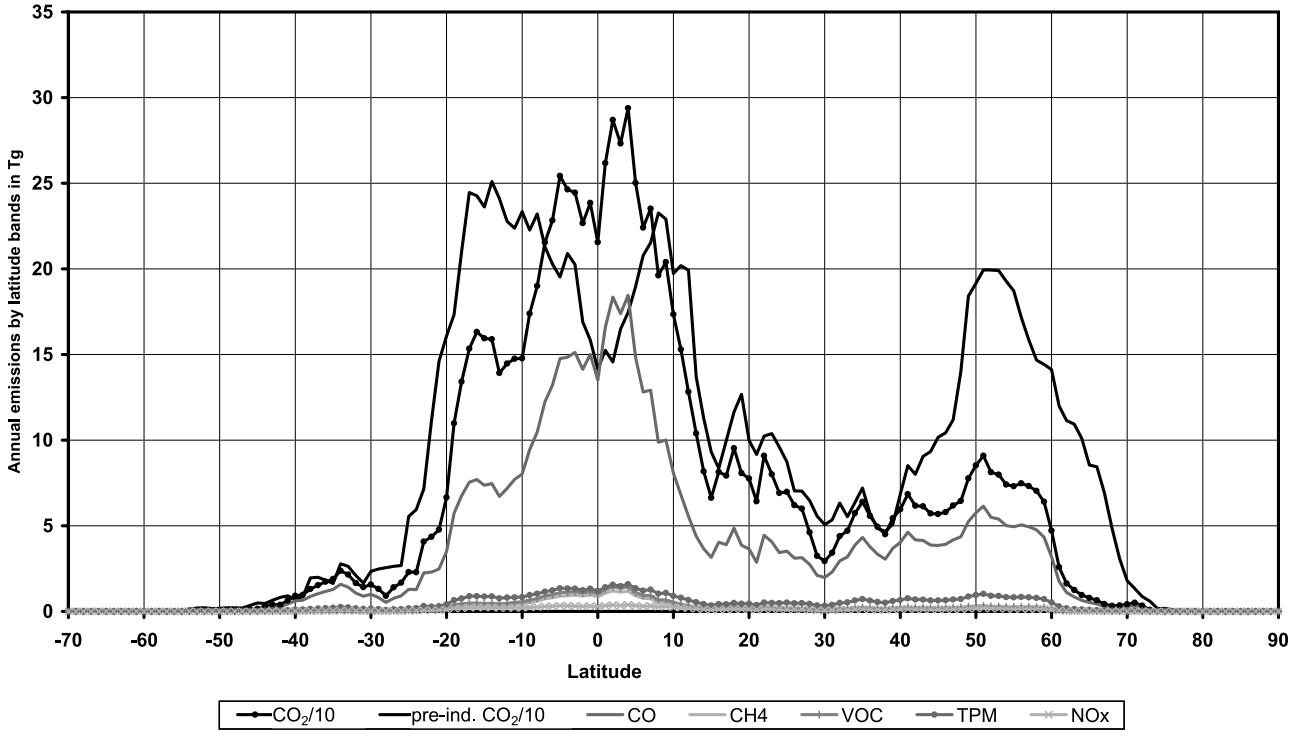

Figure 5. Latitudinal distribution of simulated trace gas emissions in the HadCM3 LGM climate (sum by latitude bands in Tg/yr).

of fire-related trace gas emission accordingly show similar patterns among LGM GCM climate data sets to those discussed for biomass burning (Table 3).

[20] The latitudinal shift of fire-related trace gas emissions could influence here atmospheric concentrations of greenhouse gases. Because we have adjusted the emission factor for NO_x to the altered LGM C:N ratio, the simulated changes in NO_x emissions show a slightly different pattern to the other trace gas emissions in low latitudes to midlatitudes (Figure 6). The propensity of NO_x to contribute to the net oxidization of other longer-lived trace gases, such as CH_4 or CO, depends on the climate conditions and convectivity of the atmosphere over the terrestrial sources of NO_x. The specific effects of changing source region for NO_x on the atmospheric conditions at the LGM will require further investigation by models that include atmospheric transport and chemistry as well as vegetation and climate.

4. Conclusion

[21] This study investigated changes in vegetation productivity, biomass burning, and associated changes in pyrogenic trace gas emissions. Simulated vegetation carbon storage was reduced by 37% under LGM conditions compared to the pre-industrial state, whereas biomass burning was reduced by only 25%. Effects of adjusting the C:N ratio to atmospheric CO_2 conditions at the LGM further intensified climate- and CO_2-induced reductions of both vegetation carbon storage and pyrogenic emissions. Environmental conditions at the LGM forced shifts of vegetation zones and decreases in woody cover. These effects are also seen in the spatial distribution of biomass burning. Changes in biomass burning and resulting trace gas emissions are dominated by a latitudinal shift toward higher emissions in the tropics rather than a reduction in global totals. The exposure of continental shelves as a result of a lower sea level contributed between 10 to 30% to increases in biomass burning in the tropics and subtropics.

[22] Volatile organic compounds, methane, and carbon monoxide are oxidized to CO_2 in a chain of chemical reactions in the troposphere. In the case of CH_4 and CO, reaction pathways differ depending on the presence of NO_x. NO_x contributes to additional OH and O_3 production, implying a higher concentration of OH radicals at the surface. Model-based investigations of atmospheric chemistry under present climate have shown that the spatial distribution of sources is important. The atmospheric lifetime of NO_x is longer in the upper troposphere than near the surface and is kept high by continued convection from surface sources [*Fuglestvedt et al.*, 2003]. Experiments with chemistry-transport models [*Fuglestvedt et al.*, 2003; *Karlsdóttir and Isaksen*, 2000] have indicated that the atmospheric oxidizing capacity is especially sensitive to changes in NO_x production in the tropics because of year-round convection that transports NO_x rapidly to high elevations. We speculate that an equatorward shift of NO_x production, which we have simulated for full-glacial conditions, might have contributed to an increased oxidizing capacity and thus to a reduced lifetime and concentration of

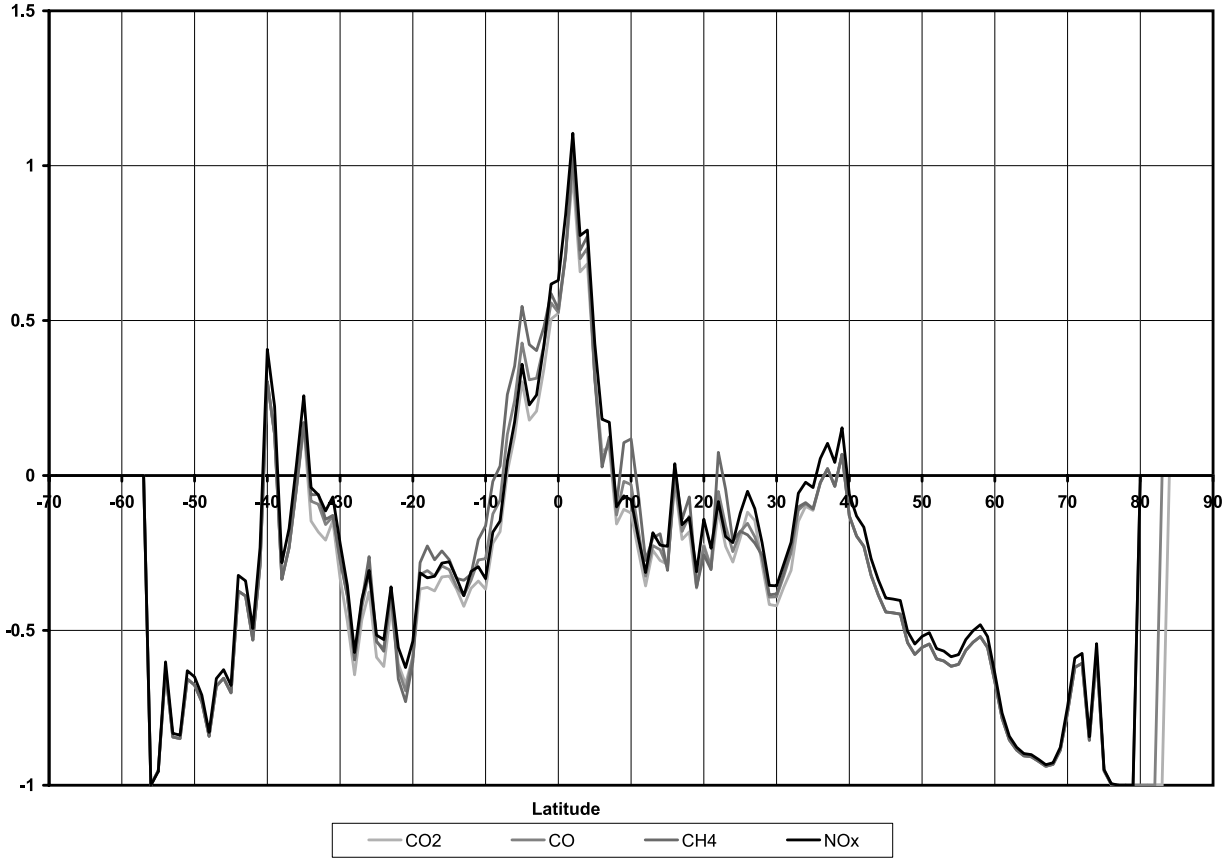

Figure 6. Changes in emissions of selected trace gases relative to pre-industrial conditions. Positive values represent more emissions under Last Glacial Maximum climate than under pre-industrial conditions, negative values the opposite. Trace gas emissions are higher in the inner tropics under LGM climate conditions than under pre-industrial condition.

CH_4, although the potential magnitude of this effect is at present quite unclear. More generally, how glacial-interglacial changes in temperature, humidity, and convective activity interacted with changes in biospheric trace gas emissions to determine the atmospheric composition is a complex question which needs to be examined further in a coupled Earth System modeling framework.

References

Anderson, R. S., and S. J. Smith (1997), The sedimentary record of fire in Montane Meadows, Sierra Nevada, California, USA: A preliminary assessment, in *Sediment Records of Biomass Burning and Global Change*, edited by J. S. Clark et al., pp. 313–327, Springer-Verlag, New York.

Andreae, M. O., and P. Merlet (2001), Emission of trace gases and aerosols from biomass burning, *Global Biogeochem. Cycles*, *15*(4), 955–966.

Bird, M. I., J. Lloyd, and G. D. Farquhar (1994), Terrestrial carbon storage at the LGM, *Nature*, *371*(6498), 566.

Bradshaw, R. H. W., K. Tolonen, and M. Tolonen (1997), Holocene records of fire from the boreal and temperate zones of Europe, in *Sediment Records of Biomass Burning and Global Change*, edited by J. S. Clark et al., pp. 347–365, Springer, New York.

Brunelle, A., and C. Whitlock (2003), Postglacial fire, vegetation, and climate history in the Clearwater Range, northern Idaho, USA, *Quat. Res.*, *60*, 307–318.

Chappellaz, J. A., I. Y. Fung, and A. M. Thompson (1993), The atmospheric CH_4 increase since the Last Glacial Maximum: 1. Source estimates, *Tellus, Ser. B*, *45*(3), 228–241.

Collatz, G. J., J. A. Berry, and J. S. Clark (1998), Effects of climate and atmospheric CO_2 partial pressure on the global distribution of C_4 grasses: Present, past, and future, *Oecologia*, *114*(4), 441–454.

Cowling, S. A., and R. Sage (1998), Interactive effects of low atmospheric CO_2 and elevated temperature on growth, photosynthesis and respiration in Phaseolus vulgaris, *Plant Cell Environ.*, *21*(4), 427–435.

Cowling, S. A., and M. T. Sykes (1999), Physiological significance of low atmospheric CO_2 for plant-climate interactions, *Quat. Res.*, *52*, 237–242.

Cowling, S. A., and M. T. Sykes (2000), Do low CO_2 concentrations affect pollen-based reconstructions of LGM climates? A response to "Physiological significance of low atmospheric CO_2 for plant-climate interactions"—Reply to Williams et al., *Quat. Res.*, *53*, 405–406.

Fuglestvedt, J. S., T. K. Berntsen, O. Godal, R. Sausen, K. P. Shine, and T. Skodvin (2003), Metrics of climate change: Assessing radiative forcing and emission indices, *Clim. Change*, *58*(3), 267–331.

Fuhrer, K., A. Neftel, M. Anklin, T. Staffelbach, and M. Legrand (1996), High-resolution ammonium ice core record covering a complete glacial-interglacial cycle, *J. Geophys. Res.*, *101*(D2), 4147–4164.

Gerten, D., S. Schaphoff, U. Haberlandt, W. Lucht, and S. Sitch (2004), Terrestrial vegetation and water balance: Hydrological evaluation of a dynamic global vegetation model, *J. Hydrol.*, *286*, 249–270.

Haberle, S. G., and M.-P. Ledru (2001), Correlations among charcoal records of fires from the past 16,000 years in Indonesia, Papua New Guinea, and Central and South America, *Quat. Res.*, *55*, 97–104.

Haberle, S. G., G. S. Hope, and S. van der Kaars (2001), Biomass burning in Indonesia and Papua New Guinea: Natural and human induced fire events in the fossil record, *Palaeogeogr. Palaeoclimatol. Palaeoecol.*, *171*(3–4), 259–268.

Hallett, D. J., D. S. Lepofsky, R. W. Mathewes, and K. P. Lertzman (2003), 11,000 years of fire history and climate in the mountain hemlock rain

forests of southwestern British Columbia based on sedimentary charcoal, *Can. J. For. Res.*, *33*(2), 292–312.

Hansson, M., and K. Holmen (2001), High-latitude biospheric activity during the last glacial cycle revealed by ammonium variations in Greenland ice cores, *Geophys. Res. Lett.*, *28*(22), 4239–4242.

Harrison, S. P., and C. I. Prentice (2003), Climate and CO_2 controls on global vegetation distribution at the Last Glacial Maximum: Analysis based on palaeovegetation data, biome modelling and palaeoclimate simulations, *Global Change Biol.*, *9*(7), 983–1004.

Hewitt, C. D., R. J. Stouffer, A. J. Broccoli, J. F. B. Mitchell, and P. J. Valdes (2003), The effect of ocean dynamics in a coupled GCM simulation of the Last Glacial Maximum, *Clim. Dyn.*, *20*, 203–218.

Jackson, S. T., R. S. Webb, K. H. Anderson, J. T. Overpeck, T. Webb III, J. W. Williams, and B. C. S. Hansen (2000), Vegetation and environment in eastern North America during the Last Glacial Maximum, *Quat. Sci. Rev.*, *19*(6), 489–508.

Joos, F., S. Gerber, I. C. Prentice, B. L. Otto-Bliesner, and P. J. Valdes (2004), Transient simulations of Holocene atmospheric carbon dioxide and terrestrial carbon since the Last Glacial Maximum, *Global Biogeochem. Cycles*, *18*, GB2002, doi:10.1029/2003GB002156.

Kageyama, M., O. Peyron, S. Pinot, P. Tarasov, J. Guiot, S. Joussaume, and G. Ramstein (2001), The Last Glacial Maximum climate over Europe and western Siberia: A PMIP comparison between models and data, *Clim. Dyn.*, *17*, 23–43.

Kaplan, J. (2002), Wetlands at the Last Glacial Maximum: Distribution and methane emissions, *Geophys. Res. Lett.*, *29*(6), 1079, doi:10.1029/2001GL013366.

Kaplan, J., I. C. Prentice, W. Knorr, and P. J. Valdes (2002), Modelling the dynamics of terrestrial carbon storage since the Last Glacial Maximum, *Geophys. Res. Lett.*, *29*(22), 2074, doi:10.1029/2002GL015230.

Karlsdóttir, S., and I. S. A. Isaksen (2000), Changing methane lifetime: Possible cause for reduced growth, *Geophys. Res. Lett.*, *27*(1), 93–96.

Kennett, J. P., and B. N. Fackler-Adams (2000), Relationship of clathrate instability to sediment deformation in the upper Neogene of California, *Geology*, *28*(3), 215–218.

Labeyrie, L., J. Cole, K. Alverson, and T. Stocker (2003), The history of climate dynamics in the Late Quaternary, in *Paleoclimate, Global Change and the Future*, edited by K. D. Alverson, R. S. Bradley, and T. F. Pedersen, pp. 33–58, Springer, New York.

Millspaugh, S. H., C. Whitlock, and P. J. Bartlein (2000), Variations in fire frequency and climate over the past 17,000 yr in central Yellowstone National Park, *Geology*, *28*(3), 211–214.

Peltier, W. R. (1994), Ice Age paleotopography, *Science*, *265*, 195–201.

Pinot, S., G. Ramstein, S. P. Harrison, I. C. Prentice, J. Guiot, M. Stute, and S. Joussaume (1999), Tropical paleoclimates at the Last Glacial Maximum: Comparison of Paleoclimate Modelling Intercomparison Project (PMIP) simulations and paleodata, *Clim. Dyn.*, *15*, 857–874.

Polley, H. W., H. B. Johnson, B. D. Marinot, and H. S. Mayeux (1993), Increase in C_3 plant water-use efficiency and biomass over Glacial to present CO_2 concentrations, *Nature*, *361*, 61–64.

Prentice, I. C., and D. Jolly (2000), Mid-Holocene and glacial-maximum vegetation geography of the northern continents and Africa, *J. Biogeogr.*, *27*(3), 507–519.

Prentice, I. C., D. Jolly, and BIOME 6000 participants (2000), Mid-Holocene and glacial-maximum vegetation geography of the northern continents, *J. Biogeogr.*, *27*, 507–519.

Sitch, S., et al. (2003), Evaluation of ecosystem dynamics, plant geography and terrestrial carbon cycling in the LPJ Dynamic Global Vegetation Model, *Global Change Biol.*, *9*, 161–185.

Thonicke, K., S. Venevsky, S. Sitch, and W. Cramer (2001), The role of fire disturbance for global vegetation dynamics: Coupling fire into a Dynamic Global Vegetation Model, *Global Ecol. Biogeogr.*, *10*(6), 661–678.

van der Kaars, S., X. Wang, P. Kershaw, F. Guichard, and D. A. Setiabudi (2000), A Late Quaternary palaeoecological record from the Banda Sea, Indonesia: Patterns of vegetation, climate and biomass burning in Indonesia and northern Australia, *Palaeogeogr. Palaeoclimatol. Palaeoecol.*, *155*(1–2), 135–153.

Wania, R., I. C. Prentice, S. P. Harrison, E. Hoornibrook, N. Gedney, T. Christensen, and R. Clymo (2004), The role of natural wetlands in the global methane cycle, *Eos Trans. AGU*, *85*(45), 466.

Williams, J. W., T. Webb, P. H. Richard, and P. Newby (2000), Late Quaternary biomes of Canada and the eastern United States, *J Biogeogr.*, *27*, 585–607.

Winkler, M. G. (1997), Late Quarternary climate, fire and vegetation dynamics, in *Sediment Records of Biomass Burning and Global Change*, edited by J. S. Clark et al., pp. 329–346, Springer-Verlag, New York.

Wooller, M. J., F. A. Street-Perrott, and A. D. Q. Agnew (2000), Late Quaternary fires and grassland palaeoecology of Mount Kenya, East Africa: Evidence from charred grass cuticles in lake sediments, *Palaeogeogr. Palaeoclimatol. Palaeoecol.*, *164*(1–4), 207–230.

C. Hewitt, Met Office, Hadley Centre, Fitz Roy Road, Exeter, Devon, EX1 3PB, UK. (chris.hewitt@metoffice.gov.uk)

I. C. Prentice, QUEST, Department of Earth Sciences, University of Bristol, Wills Memorial Building, Queen's Road, Bristol, BS8 1RJ, UK. (colin.prentice@bristol.ac.uk)

K. Thonicke, School of Geographical Sciences, University of Bristol, University Road, Bristol BS8 1SS, UK. (kirsten.thonicke@bris.ac.uk)

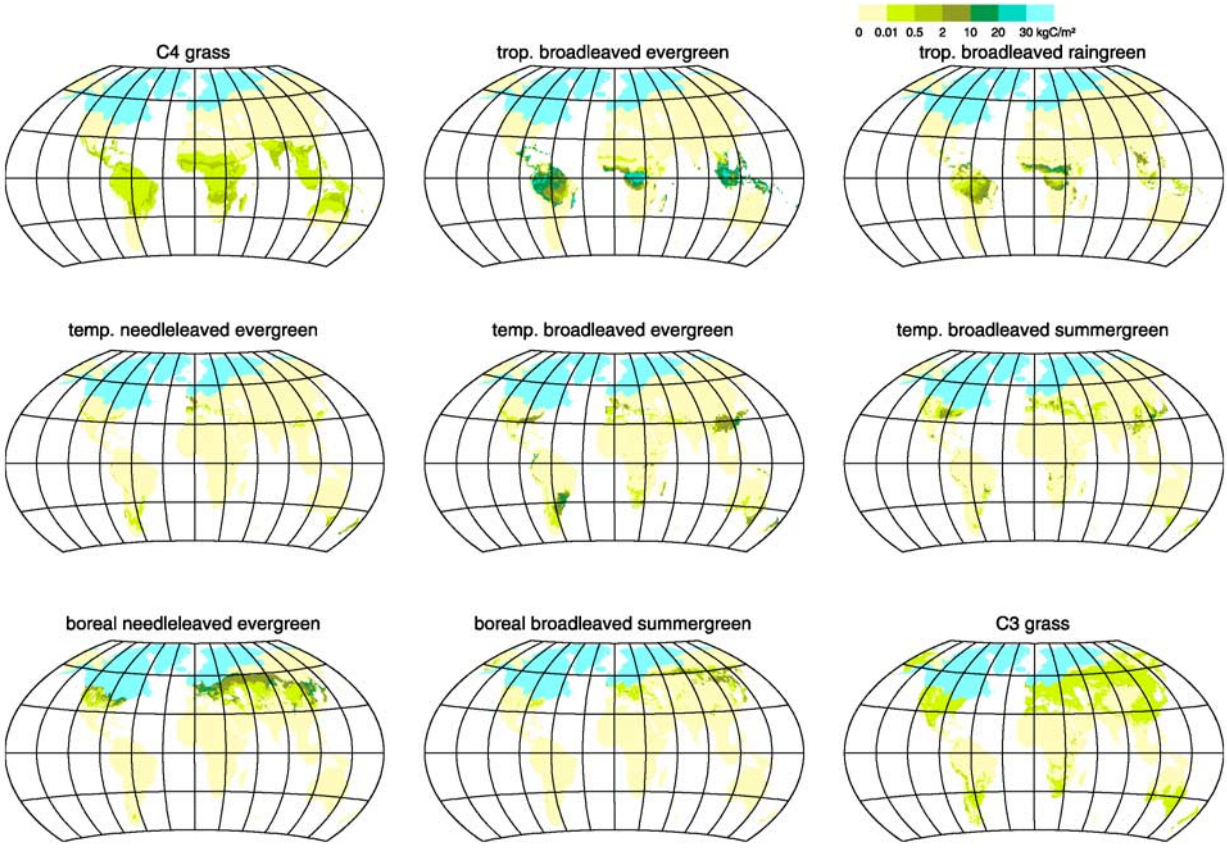

Figure 1. Carbon stored in aboveground, living biomass by Plant Functional Type (PFT). Pale blue region indicates ice. LPJ simulation uses the HadCM3 Last Glacial Maximum climate.

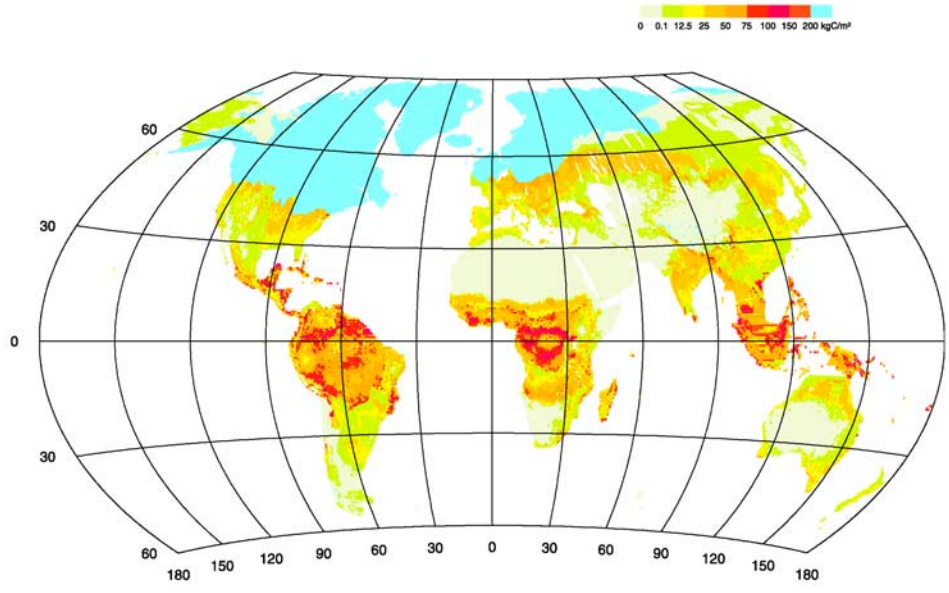

Figure 2. Simulated biomass burnt in the HadCM3 Last Glacial Maximum climate. Pale blue region indicates ice.